

# Role of the $\epsilon$ Subunit of Thermophilic $F_1$ -ATPase as a Sensor for ATP\*

Received for publication, September 7, 2007, and in revised form, October 11, 2007 Published, JBC Papers in Press, October 12, 2007, DOI 10.1074/jbc.M707509200

Shigeyuki Kato<sup>‡</sup>, Masasuke Yoshida<sup>§</sup>, and Yasuyuki Kato-Yamada<sup>‡¶1</sup>

From the <sup>‡</sup>Department of Life Science and the <sup>¶</sup>Frontier Project "Adaptation and Evolution of Extremophile," College of Science, Rikkyo (St. Paul's) University, Tokyo 171-8501, Japan and the <sup>§</sup>Chemical Resources Laboratory, Tokyo Institute of Technology, Yokohama 226-8503, Japan

The  $\epsilon$  subunit of  $F_1$ -ATPase from the thermophilic *Bacillus* PS3 (TF<sub>1</sub>) has been shown to bind ATP. The precise nature of the regulatory role of ATP binding to the  $\epsilon$  subunit remains to be determined. To address this question, 11 mutants of the  $\epsilon$  subunit were prepared, in which one of the basic or acidic residues was substituted with alanine. ATP binding to these mutants was tested by gel-filtration chromatography. Among them, four mutants that showed no ATP binding were selected and reconstituted with the  $\alpha_3\beta_3\gamma$  complex of TF<sub>1</sub>. The ATPase activity of the resulting  $\alpha_3\beta_3\gamma\epsilon$  complexes was measured, and the extent of inhibition by the mutant  $\epsilon$  subunits was compared in each case. With one exception, weaker binding of ATP correlated with greater inhibition of ATPase activity. These results clearly indicate that ATP binding to the  $\epsilon$  subunit plays a regulatory role and that ATP binding may stabilize the ATPase-active form of TF<sub>1</sub> by fixing the  $\epsilon$  subunit into the folded conformation.

$F_0F_1$ -ATPase/synthase ( $F_0F_1$ ) catalyzes ATP synthesis via coupling of the proton flow driven by the electrochemical gradient of protons or sodium.  $F_0F_1$  consists of two rotary molecular motors: a water-soluble, ATP-driven  $F_1$  motor and a membrane-embedded,  $H^+$ - or  $Na^+$ -driven  $F_0$  motor. These molecular motors are connected together to couple ATP synthesis/hydrolysis and ion flow (1–4). The  $F_1$ -ATPase ( $\alpha_3\beta_3\delta\gamma\epsilon$ ) hydrolyzes ATP into ADP and inorganic phosphate, and the hydrolysis of one ATP drives the discrete 120° rotation of the  $\gamma\epsilon$  subunits relative to the other subunits (5, 6).

As the smallest subunit of  $F_1$ -ATPase, the  $\epsilon$  subunit acts as an endogenous inhibitor of the ATPase activity in both the bacterial and chloroplast  $F_1$ -ATPase, where it is believed to play a regulatory role in ATP synthase (7–10). A recent single molecule study revealed its importance in efficient coupling in rotation and ATP synthesis (11). The  $\epsilon$  subunit consists of two distinct domains, an N-terminal  $\beta$  sandwich domain and a C-terminal  $\alpha$  helical domain. Structural and biochemical stud-

ies have shown that the  $\epsilon$  subunit adopts at least two different conformations in  $F_1$  and  $F_0F_1$  (10, 12–19). The conformation that results in the inhibition of ATPase exists in an extended state, in which the C-terminal helical domain of the  $\epsilon$  subunit unfolds to run parallel to the  $\gamma$  subunit. The conformation in which ATPase is active is known as the folded state and is characterized by C-terminal  $\alpha$  helices folded into a hairpin configuration. The conformational change of the  $\epsilon$  subunit is controlled by the concentration of both ATP and ADP as well as the membrane potential (16–19).

The isolated  $\epsilon$  subunit of  $F_1$  from the thermophilic *Bacillus* strain PS3 (TF<sub>1</sub>)<sup>2</sup> was recently found to bind ATP (20). Binding was so specific that GTP and ADP failed to form a complex with the  $\epsilon$  subunit, as assayed by gel filtration. These results led to the suggestion that the  $\epsilon$  subunit is both a regulator and sensor of cellular ATP concentration. ATP binding was also observed with the  $\epsilon$  subunits of  $F_1$ -ATPases from *Bacillus subtilis* (21) and *Escherichia coli* (22). X-ray crystallographic analysis revealed that ATP is bound to the  $\epsilon$  subunit in the folded state (22). As the ATP binding site consists of residues from the N-terminal domain and the first and second  $\alpha$  helices of the C-terminal domain, ATP may bind to the  $\epsilon$  subunit alone in the folded state. An NMR study revealed that in the absence of ATP, the  $\epsilon$  subunit adopts a different conformation. ATP may stabilize the folded conformation of the  $\epsilon$  subunit (22). ATP binding was also observed with the  $\epsilon$  subunit in the  $\gamma\epsilon$  subcomplex, indicating that ATP binding to the  $\epsilon$  subunit can occur in ATP synthase, in which it may play a regulatory role (23).

To determine the role of ATP binding to the  $\epsilon$  subunit in the regulation of the  $F_0F_1$ -ATP synthase, 11 mutants of the  $\epsilon$  subunit were constructed, in which basic or acidic residues were substituted with alanine residues. Several mutants with impaired ATP binding were further reconstituted with  $\alpha_3\beta_3\gamma$ , and the ATPase activities of these  $\alpha_3\beta_3\gamma\epsilon$  complexes were measured. The results clearly show that ATP binding to the  $\epsilon$  subunit affects the regulation of ATPase activity.

\* This work was supported in part by Grants-in-aid for Scientific Research on Priority Areas (18074002) and for Young Scientists (18770118) from the Ministry of Education, Culture, Sports, Science, and Technology of Japan and the Rikkyo University Special Fund for Research (to Y. K.-Y.). The costs of publication of this article were defrayed in part by the payment of page charges. This article must therefore be hereby marked "advertisement" in accordance with 18 U.S.C. Section 1734 solely to indicate this fact.

<sup>1</sup> To whom correspondence should be addressed: Dept. of Life Science, College of Science, Rikkyo (St. Paul's) University, 3-34-1 Nishi-Ikebukuro, Toshima-ku, Tokyo 171-8501, Japan. Tel.: 81-3-3985-2386; Fax: 81-3-3985-2386; E-mail: katoyama@rikkyo.ac.jp.

<sup>2</sup> The abbreviations used are: TF<sub>1</sub>,  $F_1$ -ATPase from thermophilic *Bacillus* PS3; BF<sub>1</sub>,  $F_1$ -ATPase from *B. subtilis*; EF<sub>1</sub>,  $F_1$ -ATPase from *E. coli*; IC3-PE-maleimide, N-ethyl-N'-[5-[N''-(2-maleimidoethyl)pyperazinocarbonyl]pentyl]indocarbocyanine; WT, wild type; TES, 2-[[2-hydroxy-1,1-bis(hydroxymethyl)ethyl]amino]ethanesulfonic acid; AMP-PNP, 5'-adenylyl- $\beta$ , $\gamma$ -imidodiphosphate.

## EXPERIMENTAL PROCEDURES

**Materials**—Wild-type and  $\alpha$ K175A/T176A mutant (noncatalytic site-deficient mutant,  $\Delta$ NC)<sup>3</sup>  $\alpha_3\beta_3\gamma$  complexes of  $TF_1$  were prepared as described previously (24, 25). An expression plasmid for a mutant  $\alpha_3\beta_3\gamma$  complex was prepared containing KT/AA substitutions in Walker A motifs (27) in both the  $\alpha$  and  $\beta$  subunits ( $\alpha$ K175A/T176A and  $\beta$ K164A/T165A, noncatalytic and catalytic site-deficient mutants,  $\Delta$ NC/ $\Delta$ C); a DNA fragment containing the  $\beta$ K164A/T165A mutations was prepared using the overlap extension PCR method (28, 29) applied to the expression plasmid for the wild-type (WT)  $\alpha_3\beta_3\gamma$  complex. A 900-bp fragment containing mutations was treated with restriction enzymes AgeI and MunI, and the resulting 624-bp fragment was purified and directly transferred to the respective sites of an expression plasmid for the  $\Delta$ NC ( $\alpha$ K175A/T176A) mutant  $\alpha_3\beta_3\gamma$  complex. The mutant  $\alpha_3\beta_3\gamma$  complex was purified in the same way as the wild-type complex. The wild-type and S48C/N125C mutant ( $\epsilon^{NCX}$ , a mutant  $\epsilon$  subunit of  $TF_1$  in which N- and C-terminal domains can be cross-linked)  $\epsilon$  subunits were prepared as previously described (16, 30). The expression plasmids for the mutant  $\epsilon$  subunits were prepared by the overlap extension PCR method or mega-primer PCR method (31) applied to the pET21/ $TF_1$ - $\epsilon$  (wild-type) plasmid (20). The Q107C mutation for fluorescent labeling was introduced by the mega-primer PCR method applied to the expression plasmid for the mutants deficient in ATP binding. Mutations were confirmed by DNA sequencing. Except for the E83A and E83A/Q107C mutants, the  $\epsilon$  subunits were prepared as described previously (16, 30). It was noticed that the use of a large sized butyl-TOYOPEARL column resulted in a reduced amount of bound ATP in the  $\epsilon$  subunit preparation, reaching <0.05 mol/mol (23). The E83A mutant  $\epsilon$  subunit was prepared as follows. Cells were suspended in 50 mM Tris-HCl (pH 8) and 1 mM EDTA (buffer A) and disrupted by French press. Cell lysate was ultracentrifuged at  $220,000 \times g$  for 1 h at 4 °C. The supernatant was applied to a DEAE-TOYOPEARL column equilibrated with the same buffer. As the mutant  $\epsilon$  subunit was adsorbed on the column, a 0–100 mM linear gradient of NaCl was applied, and the fractions containing  $\epsilon$  subunit were pooled. Solid ammonium sulfate was added to the sample to 20% saturation, and the sample was applied to a phenyl-TOYOPEARL column equilibrated with buffer A containing a 25% saturated concentration of ammonium sulfate. Proteins were eluted with a 25 to 0% saturation linear gradient of ammonium sulfate. For purification of the E83A/Q107C mutant, 1 mM dithiothreitol was included in all buffers. The  $\alpha_3\beta_3\gamma\epsilon$  complex was prepared by mixing the purified  $\alpha_3\beta_3\gamma$  complex and  $\epsilon$  subunit to a molar ratio of 1:10 (10). Excess  $\epsilon$  subunit was not removed for the ATPase measurements. For the experiments in Fig. 6, excess  $\epsilon$  subunit was removed from the  $\alpha_3\beta_3\gamma\epsilon$  complex by three successive ultrafiltrations (100-kDa cutoff) with an Amicon centrifugal filter device as described previously (16). Formation of the  $\alpha_3\beta_3\gamma\epsilon$  complex was confirmed by polyacrylamide gel electrophoresis without a denaturing reagent.

<sup>3</sup> As noted in Ref. 26,  $\alpha$ K175A/T176A mutations are enough to suppress the nucleotide binding to the noncatalytic site.

**ATP Binding Assay**—ATP binding assay by gel-filtration chromatography on a Sephadex G25F column (GE Healthcare) was performed as reported previously in a buffer consisting of 50 mM Tris-HCl (pH 8) and 100 mM KCl at room temperature (25 °C) (20). ATP binding assay by fluorescence was performed as described above (19) except that *N*-ethyl-*N'*-[5-[*N''*-(2-maleimidoethyl)piperazinocarbonyl]pentyl]indocarbocyanine (IC3-PE-maleimide; Dojin) was used instead of Cy3-maleimide. Labeling was performed in 50 mM TES-NaOH (pH 7) and 100 mM NaCl with a protein-to-dye ratio of 1:2–7. Excess dye was removed with a Bio-Gel P6 centrifuge column (Bio-Rad). The assay mixture contained 50 mM HEPES-KOH (pH 7.5), 100 mM KCl, and 10 mM MgCl<sub>2</sub>. Fluorescently labeled  $\epsilon$  subunit (100 nM) was incubated in the assay mixture, and the changes in fluorescence were measured upon addition of ATP. The measurements were performed at 25 °C with an FP-6500 fluorescent spectrometer (JASCO). Excitation and emission wavelengths were 522 and 559 nm, respectively. Slit widths for excitation and emission were 3 nm. Fluorescent change was corrected for corresponding measurement without ATP and plotted against ATP concentration.

**ATPase Assay**—ATPase activity was measured spectrophotometrically with an NADH-coupled ATP-regenerating system at 25 °C (32). The assay mixture consisted of 50 mM Tris-HCl (pH 8), 100 mM KCl, 2.5 mM phosphoenolpyruvate, 2 mM MgCl<sub>2</sub>, 0.2 mM NADH, 50  $\mu$ g/ml pyruvate kinase, 50  $\mu$ g/ml lactate dehydrogenase, and the indicated concentration of ATP-Mg. The reaction was initiated by the addition of 10 nM  $TF_1$   $\alpha_3\beta_3\gamma\epsilon$  complex to the assay mixture, and changes in absorbance at 340 nm were measured in a V-550 or V-530 spectrophotometer (JASCO). Velocity measurements were taken at 540–1140 s after the start of the reactions. One unit of ATPase activity was defined as that producing 1  $\mu$ mol of ADP/min.

**Detection of Conformation of the  $\epsilon$  Subunit**—The detection of a conformational change in the  $\epsilon$  subunit corresponding to the formation of an intramolecular disulfide bond was performed in essentially the same way as described previously (16). Reduced  $\Delta$ NC/ $\Delta$ C- $\alpha_3\beta_3\gamma\epsilon^{NCX}$  and  $\Delta$ NC- $\alpha_3\beta_3\gamma\epsilon^{NCX}$  complexes were incubated with or without 2 mM ATP-Mg. After 10 min, 0, 10, 20, or 50  $\mu$ M CuCl<sub>2</sub> was added, and the sample was incubated for 1 h at room temperature. The cross-linking reaction was quenched by addition of 10 mM EDTA. IC3-PE-maleimide (500  $\mu$ M) and 0.1% SDS were then added to the mixture and incubated for 10 min at room temperature to label cysteine residues that had not formed a disulfide bond. The reaction was quenched by the addition of 12 mM *N*-ethylmaleimide. The samples were analyzed by SDS-PAGE without reducing reagent (15% polyacrylamide). The fluorescent image was taken by a Typhoon 9210 image analyzer (GE Healthcare) with a green laser (532 nm) and an appropriate filter set. The gel was then stained with Coomassie Brilliant Blue R-250, and the image was recorded with a GT-9800F flatbed scanner (Epson). As judged by the gel-filtration analysis, no difference in ATP binding was observed between the mutant  $\epsilon^{NCX}$  subunit and the wild-type (data not shown).

**Re-inactivation Assay**—Re-inactivation of the  $\alpha_3\beta_3\gamma\epsilon$  complex by lowering the ATP concentration was measured as follows. The  $\alpha_3\beta_3\gamma\epsilon$  complex was incubated with 4 mM ATP-Mg



## ATP Binding to the $\epsilon$ Subunit of $F_1$ -ATPase

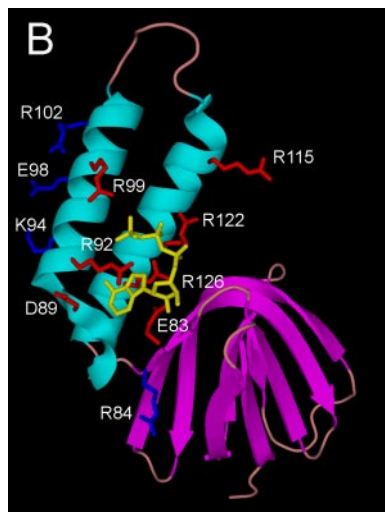
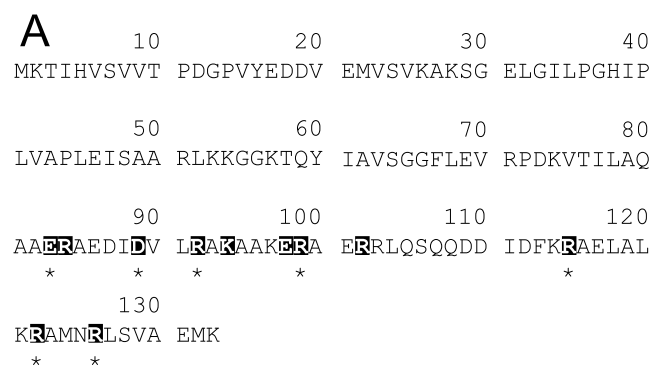


**FIGURE 1. Positions of the mutations.** *A*, the primary structure of the  $\epsilon$  subunit. The mutated residues are highlighted. Residues chosen from the interactions with ATP in the crystal structure are marked with *asterisks*. *B*, crystal structure of the  $\epsilon$  subunit-ATP complex. ATP is shown in yellow. Mutated residues are shown in blue and red; the former are selected from differences between  $TF_1$  and  $BF_1$ , whereas the latter are from the crystal structure. This figure was generated with PyMOL (DeLano Scientific) from chain A of Protein Data Bank code 2E5Y.

in a buffer consisting of 50 mM Tris-HCl (pH 8), 100 mM KCl, and 2 mM  $MgCl_2$  at 25 °C for more than 10 min. Bovine serum albumin (0.1 mg/ml) was included in the control measurement, which was carried out with the  $\alpha_3\beta_3\gamma$  complex. Five  $\mu$ l of the mixture was then added to 1 ml of ATPase assay mixture without ATP in a quartz cuvette to give a final concentration of ATP at 20  $\mu$ M.

**Other Methods**—Protein concentrations of the  $\epsilon$  subunits were determined by the method of Bradford (33) using bovine serum albumin as a standard and corrected by multiplying by a factor of 0.54 according to the results of amino acid quantification (20). Concentrations of  $\alpha_3\beta_3\gamma$  or  $\alpha_3\beta_3\gamma\epsilon$  complexes were determined by measuring UV absorption spectra using  $A_{280} = 0.45$  at 1 mg/ml (25). Chemicals were of the highest grades available.

## RESULTS AND DISCUSSION

**Altered ATP Binding to the Mutant  $\epsilon$  Subunits**—To obtain  $\epsilon$  subunit mutants that showed altered ATP binding, alanine-based substitutions were carried out (highlighted in Fig. 1*A*) for the following reasons: 1) These are the basic or acidic residues present in the C-terminal domain that are different in  $TF_1$  and

$BF_1$ . Although ATP binding to the  $\epsilon$  subunit of  $BF_1$  was observed, the affinity for ATP was greatly reduced (21). One possibility is that these residues may be responsible for the difference (R84A, K94A, E98A, and R102A, shown in blue in Fig. 1*B*). 2) These are the residues that formed hydrogen bonds with ATP in the crystal structure of the  $TF_1$   $\epsilon$  subunit-ATP complex (E83A, D89A, R92A, R99A, R115A, R122A, and R126A, marked with *asterisks* in Fig. 1*A* and shown in red in Fig. 1*B*), although two of these (Arg<sup>122</sup> and Arg<sup>126</sup>) were thought to play an inhibitory role in a previous study (34). Arg<sup>115</sup> appeared to interact with ATP bound to another monomer  $\epsilon$  subunit in the crystal structure (22) and, possibly, to be involved in ATP binding. ATP binding to these mutants was assayed by gel-filtration chromatography. The results are shown in Fig. 2. Two mutants (R102A and R115A) showed essentially the same profile as the wild type. Four (E83A, R92A, R122A, and R126A) showed no ATP binding, and the other five (R84A, D89A, K94A, E98A, and R99A) showed a moderate degree of binding. For further analyses, four mutants (E83A, R92A, R122A, and R126A) were chosen that showed virtually no ATP binding in the gel-filtration assay. Interestingly, all these residues are conserved between  $TF_1$  and  $BF_1$ . Arg<sup>92</sup>, which was included in the previously proposed consensus ATP binding motif, I(L)DXXRA, was found to be important for ATP binding (22). As determined previously, Glu<sup>83</sup> was also found to be important for ATP binding (22). The mutants selected by the differences between  $TF_1$  and  $BF_1$  had a relatively minor effect on ATP binding. The difference in ATP binding between  $TF_1$  and  $BF_1$  may be because of the differences in other residues. As for *E. coli*  $F_1$ -ATPase ( $EF_1$ )  $\epsilon$ , only Arg<sup>92</sup> is conserved, although  $EF_1$   $\epsilon$  possesses a lysine residue in place of Arg<sup>122</sup>. These differences may be the cause of the very weak affinity for ATP of the  $EF_1$   $\epsilon$  subunit (22). The cysteine residue introduced at Gln<sup>107</sup>, located in the loop region between the two C-terminal  $\alpha$  helices, was labeled with fluorescent maleimide. This was used to provide a more accurate measurement of the ATP binding affinity of the mutants that showed no ATP binding in the gel-filtration analysis. Although the extent of fluorescence varied with mutants, possibly because of the differences in the interactions between dye and protein, saturating ATP concentration dependence of the fluorescence was observed (Fig. 3). The  $K_d$  for ATP at 25 °C of these mutants varied from 100  $\mu$ M to >1 mM. Although the crystal structure suggests that the Glu<sup>83</sup> and Arg<sup>92</sup> residues are important for ATP binding, the mutation at Arg<sup>126</sup> was shown to have a more significant effect.

**Suppressed ATPase Activity with Mutant  $\epsilon$  Subunits**—There was no significant difference in ATPase activities of  $\alpha_3\beta_3\gamma\epsilon$  complexes containing mutant  $\epsilon$  subunit at high ATP concentration (2 mM) (Fig. 4*A*). However, reduction in ATP concentration resulted in more prominent differences in mutant ATPase activities. For example, at 200  $\mu$ M ATP (Fig. 4*B*),  $\alpha_3\beta_3\gamma\epsilon$  complexes containing R126A showed markedly lower ATPase activity than the wild-type complex. At 20  $\mu$ M ATP (Fig. 4*C*), the differences were more significant, and the  $\alpha_3\beta_3\gamma\epsilon$  complex containing E83A or R92A also showed a reduction in ATPase activity compared with the wild-type complex. The ATP concentration dependence of the ATPase activity is summarized in Fig. 5. The ATP concentration that resulted in half-

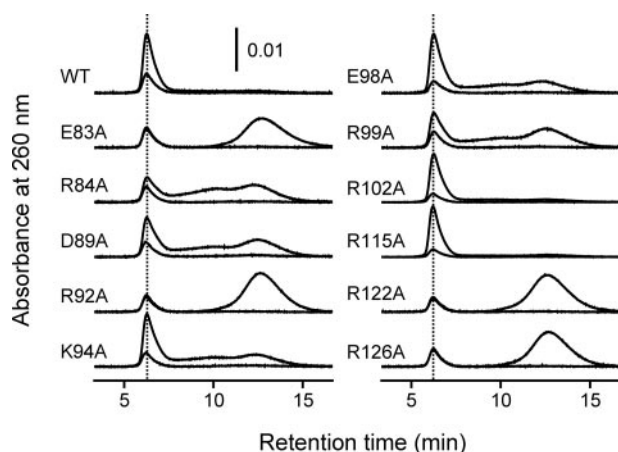


**FIGURE 2. Gel-filtration analysis of ATP binding to the mutant  $\epsilon$  subunits of  $TF_1$ .** ATP binding to the mutant  $\epsilon$  subunits ( $25 \mu\text{M}$ ) was analyzed on a Sephadex G25F column. Elution was monitored at 260 nm. Mutations are described on the left of each trace. Upper and lower traces represent measurements with and without  $25 \mu\text{M}$  ATP, respectively. Positions of the peaks containing  $\epsilon$  subunit are marked with dotted lines. The vertical bar on top of the figure represents 0.01 absorbance unit at 260 nm. Other experimental conditions are described under "Experimental Procedures."

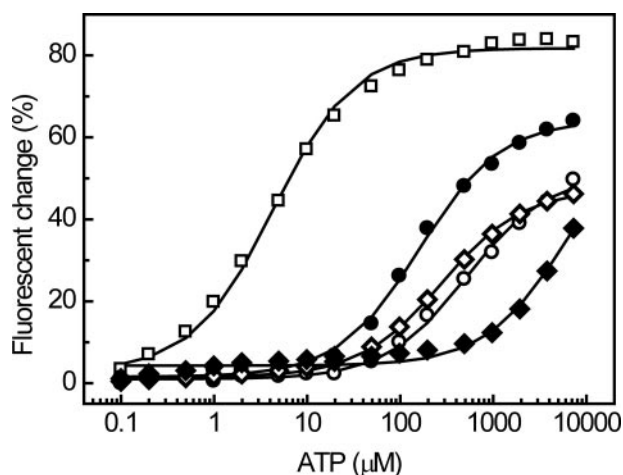


**FIGURE 3. Affinity of the mutant  $\epsilon$  subunits for ATP.** Changes in the fluorescence of IC3-labeled mutant  $\epsilon$  subunits upon addition of ATP were measured. ATP was added to the IC3-labeled  $\epsilon$  subunit sequentially. Changes in fluorescence are corrected for corresponding measurements without ATP, normalized to initial fluorescence, and plotted against ATP concentration. Excitation and emission wavelengths were 522 and 559 nm, respectively. Open square, open circle, closed circle, open diamond, and closed diamond represent wild type, E83A, R92A, R122A, and R126A, respectively. Lines represent fits with data by a simple binding scheme. Calculated  $K_d$  values and maximum fluorescence of the mutants for ATP are as follows:  $4.3 \mu\text{M}$ , 79% (wild type);  $520 \mu\text{M}$ , 50% (E83A);  $160 \mu\text{M}$ , 63% (R92A);  $280 \mu\text{M}$ , 46% (R122A); and  $>1000 \mu\text{M}$ , 61% (R126A), respectively.

maximum activity may not directly relate to the  $K_d$  for ATP of the  $\epsilon$  subunit because activity was measured at a defined time point and not at final equilibrium. However, with the exception of R122A, increased inhibition was observed with less ATP binding mutant  $\epsilon$  subunit (Fig. 5B). The strengths of ATP binding were in the following order: WT  $>$  R92A  $>$  R122A  $>$  E83A  $>$  R126A, whereas the activities were in the following order: R122A  $>$  WT  $>$  R92A  $>$  E83A  $>$  R126A. The exceptional behavior of R122A may be because of the direct involvement of Arg<sup>122</sup> in the inhibitory effect of the  $\epsilon$  subunit itself (34).

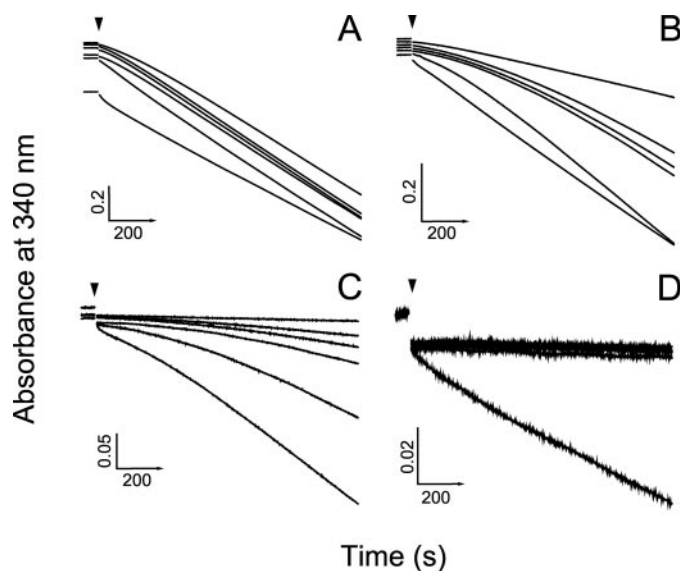


**FIGURE 4. Time courses of ATP hydrolysis by the  $\alpha_3\beta_3\gamma$  complex with mutant  $\epsilon$  subunits.** ATPase activities were measured with an NADH-coupled ATP-regenerating system at  $25^\circ\text{C}$ . Changes in the absorbance at 340 nm are plotted against time. In each panel, traces represent, from top to bottom,  $\alpha_3\beta_3\gamma$  complexes with mutant  $\epsilon$  subunits: R126A, E83A, R92A, WT, R122A, and  $\alpha_3\beta_3\gamma$  complex, respectively. ATP concentrations were  $2 \text{ mM}$  (A),  $200 \mu\text{M}$  (B),  $20 \mu\text{M}$  (C), and  $2 \mu\text{M}$  (D). Vertical bars in each panel represent the absorbance unit on the left. Horizontal arrows indicate 200 s.  $\alpha_3\beta_3\gamma$  complexes were added at the time indicated by arrowheads. Other experimental conditions are described under "Experimental Procedures."

**ATP Binding to the  $\epsilon$  Subunit Is Not a Primary Event in Activation**—In a previous study, nucleotide binding to the  $\beta$  subunit was found to be responsible for the conformational change in the  $\epsilon$  subunit because the conformational change was also observed in the noncatalytic site-deficient mutant ( $\Delta\text{NC}$ ); in addition, it was noted that AMP-PNP could also induce conformational change in the  $\epsilon$  subunit (16). However, the finding that the  $\epsilon$  subunit can bind ATP raises the possibility that ATP binding may be a trigger for the conformational change in the  $\epsilon$  subunit. To test this hypothesis, a mutant  $\alpha_3\beta_3\gamma$  complex was prepared that contained KT/AA substitutions in Walker A motifs (27) in both the  $\alpha$  and  $\beta$  subunits ( $\Delta\text{NC}/\Delta\text{C}$ ). The KT/AA mutations are known to result in the loss of ATP binding in several Walker-type ATPases (25, 35). The  $\Delta\text{NC}/\Delta\text{C}$ - $\alpha_3\beta_3\gamma$  complex showed no steady-state ATPase activity (that is, less than 1/100 of  $\Delta\text{NC}$ , i.e.  $<1/10000$  of the wild type) despite the presence of 0.3% lauryldimethylamine oxide. This suggests that virtually no ATP was bound to the catalytic sites (data not shown). In Fig. 6, a decrease in the fluorescent band indicated that the  $\epsilon$  subunit was adopting a folded state, thus easily forming a cross-link between S48C and N125C. With the  $\Delta\text{NC}$  mutant, ATP-dependent enhancement of the cross-link formation in the  $\epsilon^{\text{NCX}}$  subunit was observed (Fig. 6) (16). In contrast, no enhancement of cross-link formation was observed with the  $\Delta\text{NC}/\Delta\text{C}$  mutant (Fig. 6). The results implied that ATP does not bind primarily to the  $\epsilon$  subunit, but rather to the (possibly second or third) catalytic site(s). This may be the trigger for activation from inhibition by the  $\epsilon$  subunit. When the  $\epsilon$  subunit is in the extended state, the ATP binding site is divided, and ATP cannot access the residues therein as they are hidden within the  $\alpha_3\beta_3$  cavity. ATP binding to the  $\beta$  subunit may



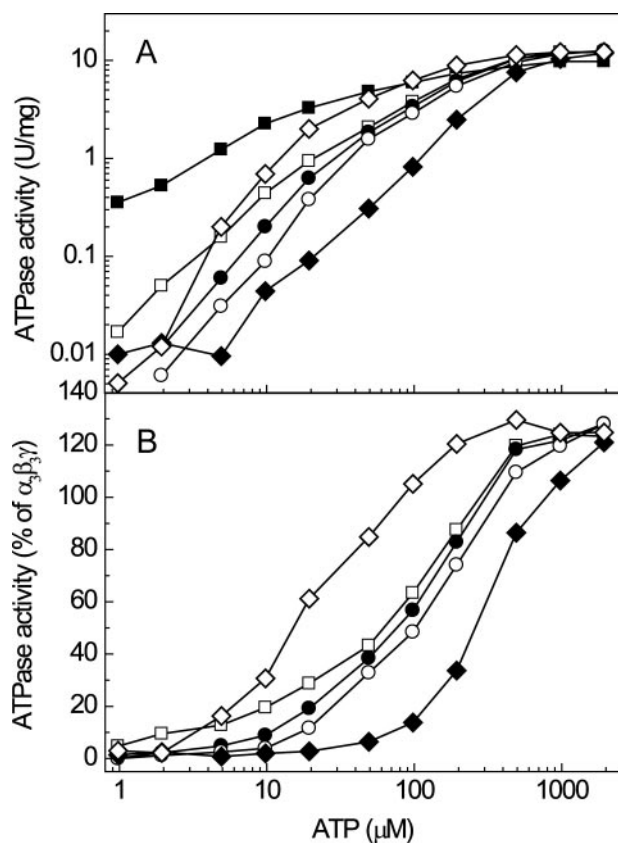


**FIGURE 5. ATP concentration dependence of the ATPase activity.** A, ATPase activities of the  $\alpha_3\beta_3\gamma\epsilon$  complexes are plotted against ATP concentration. Velocities were taken at 540–1140 s after the initiation of the reactions. Closed square, open square, open circle, closed circle, open diamond, and closed diamond represent  $\alpha_3\beta_3\gamma\epsilon$  complexes with mutant  $\epsilon$  subunits: none ( $\alpha_3\beta_3\gamma$  complex), wild type, E83A, R92A, R122A, and R126A, respectively. B, ATPase activities of the  $\alpha_3\beta_3\gamma\epsilon$  complexes are normalized to that of the  $\alpha_3\beta_3\gamma$  complex at each ATP concentration. Symbols are the same as in A.

induce conformational changes in the  $\beta$  subunit, resulting in expulsion of the  $\epsilon$  subunit from the  $\alpha_3\beta_3$  cylinder. Once the C-terminal helices are expelled from the  $\alpha_3\beta_3$  cylinder, ATP can access the binding site on the  $\epsilon$  subunit.

**Re-inactivation by Decreasing ATP Concentration**—At high concentrations of ATP (e.g. 2 mM) (Fig. 4A), the ATPase activities of the  $\alpha_3\beta_3\gamma\epsilon$  complexes containing the wild-type or mutant  $\epsilon$  subunit were found to be similar. However, the ATPase activities differed significantly at low concentrations of ATP (e.g. 20  $\mu$ M) (Fig. 4C). Following from this, the ATP concentration was changed from high to low to determine the impact of ATP dissociation from the  $\epsilon$  subunit in the  $\alpha_3\beta_3\gamma\epsilon$  complex. The  $\alpha_3\beta_3\gamma\epsilon$  complex was incubated with 4 mM ATP-Mg for more than 10 min at room temperature. As reported previously, this treatment activated the  $\alpha_3\beta_3\gamma\epsilon$  complex (10). Five  $\mu$ l of the sample was then injected into 1 ml of ATP-free ATPase assay mixture to give a final ATP concentration of 20  $\mu$ M. In contrast to the ATPase measurement taken without preincubation with ATP (Fig. 4C), the WT  $\alpha_3\beta_3\gamma\epsilon$  complex showed similar ATPase activity to the  $\alpha_3\beta_3\gamma$  complex (Fig. 7). Slow inactivation was observed with E83A, R92A, and R126A, for which the  $K_d$  for ATP was higher than 20  $\mu$ M. The reason ATPase activity remained high in the WT  $\alpha_3\beta_3\gamma\epsilon$  complex may have been because the wild-type  $\epsilon$  subunit maintained

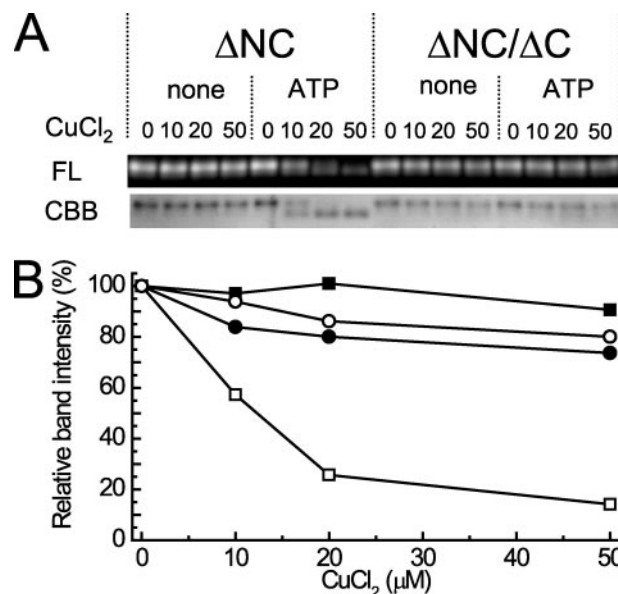


**FIGURE 6. Effect of ATP on formation of the cross-link in the  $\epsilon$  subunit.** A, the  $\Delta$ NC- and  $\Delta$ NC/ $\Delta$ C- $\alpha_3\beta_3\gamma\epsilon^{NCX}$  complexes were incubated with 4 mM ATP-Mg. Cross-linking was induced by the addition of  $\text{CuCl}_2$  (0, 10, 20, or 50  $\mu$ M as indicated). After 1 h, non-cross-linked sulfhydryl groups were labeled with IC3-PE-maleimide. The samples were then separated by 15% SDS-PAGE without reducing agent. The fluorescent image of the gel was taken by a Typhoon 9210 image analyzer (FL, upper panel) and then stained with Coomassie Brilliant Blue R-250 (CBB, lower panel). Only the region around the  $\epsilon$  subunit is shown. B, the band intensities of the fluorescent image in A are quantified and plotted against  $\text{CuCl}_2$  concentration. Closed square, open square, closed circle, and open circle represent  $\Delta$ NC without ATP,  $\Delta$ NC with ATP,  $\Delta$ NC/ $\Delta$ C without ATP, and  $\Delta$ NC/ $\Delta$ C with ATP, respectively.

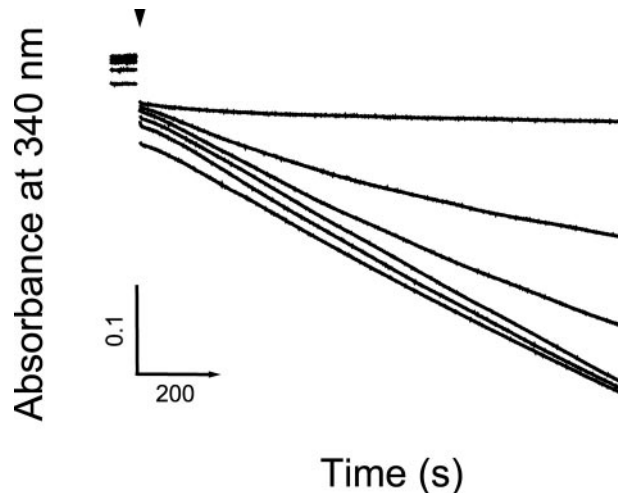


**FIGURE 7. Re-inactivation of  $\alpha_3\beta_3\gamma\epsilon$  complexes by lowering ATP concentration.** The  $\alpha_3\beta_3\gamma\epsilon$  complexes were incubated with 4 mM ATP-Mg. After more than 10 min of incubation, 5  $\mu$ l of the mixture was injected at the time indicated by the arrowhead into 1 ml of assay mixture without ATP to give the final concentration of ATP, 20  $\mu$ M. Traces represent, from top to bottom,  $\alpha_3\beta_3\gamma\epsilon$  complexes with mutant  $\epsilon$  subunits: R126A, E83A, R92A, WT, R122A, and  $\alpha_3\beta_3\gamma$  complex, respectively. The vertical bar represents 0.1 absorbance unit at 340 nm. The horizontal arrow indicates 200 s.  $\alpha_3\beta_3\gamma\epsilon$  complexes were added at the time indicated by the arrowhead. Other experimental conditions are described under "Experimental Procedures."

high affinity for ATP, and thus ATP remained bound even at a concentration of 20  $\mu$ M.

**ATP Binding to the  $\epsilon$  Subunit Shifts the Equilibrium between Inactive and Active States**—The ATP binding form of the  $\epsilon$  subunit was revealed as the folded state (22). The binding site

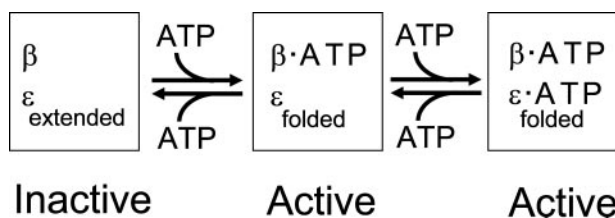


FIGURE 8. **Schematic model of regulation by and ATP binding to the  $\epsilon$  subunit.** In the absence of ATP, the  $\alpha_3\beta_3\gamma\epsilon$  complex adopts the inactive state. ATP binding to the  $\beta$  subunit(s) induces activation, accompanying conformational changes in the  $\epsilon$  subunit. Once the  $\epsilon$  subunit adopts the folded conformation, ATP can bind to the  $\epsilon$  subunit. ATP binding to the  $\epsilon$  subunit stabilizes the ATPase-active folded state of the  $\alpha_3\beta_3\gamma\epsilon$  complex. See "Results and Discussion" for details.

consists of both the N- and C-terminal domains. Moreover, there may be no room for ATP to bind to the  $\epsilon$  subunit in the extended form, as the C-terminal helices of the  $\epsilon$  subunit are surrounded by the  $\alpha$ ,  $\beta$ , and  $\gamma$  subunits. The results also imply that fluctuation of the  $\epsilon$  subunit between folded and extended forms rarely occurs in the absence of ATP binding to the  $\beta$  subunits. The likely role of ATP binding to the  $\epsilon$  subunit is to stabilize the  $\epsilon$  subunit of activated complex in the folded state. A simplified model is shown in Fig. 8. The ATPase-inactive  $TF_1$  complex is activated by binding of ATP to the  $\beta$  subunit(s). Upon activation, the  $\epsilon$  subunit changes its conformation from the extended to the folded state. However, in the absence of bound ATP, the folded state is unstable (22), and the C-terminal domain of the  $\epsilon$  subunit has the tendency to return to its extended form. ATP binding to the  $\epsilon$  subunit stabilizes the folded state, shifts the equilibrium between the inactive and active states of  $TF_1$ , and results in a higher proportion of active complex. This may be important when, for example, cells contain sufficient ATP, but the membrane potential is low because of an alkaline environment. Under such conditions,  $F_0F_1$  may work as a proton pump to build up membrane potential at the expense of ATP. In the absence of ATP binding to the  $\epsilon$  subunit, however,  $F_0F_1$  may readily adopt the ATPase-inactive conformation even if the cell contains sufficient ATP. It should be noted that affinity for ATP of the  $\epsilon$  subunit under physiological temperature is relatively low ( $K_d = 0.6$  mM at 65 °C), and the cellular ATP concentration may fluctuate in this range (19). In the case of  $BF_1$ , because the  $K_d$  for ATP is in the order of mM (21), the regulatory mechanism may be the same as that of  $TF_1$ . As for  $EF_1$ , the  $K_d$  value of  $\epsilon$  was reported to be 22 mM at 25 °C (22), and this low affinity for ATP may be the cause of the strong inhibitory effect of  $EF_1$   $\epsilon$  compared with that of  $TF_1$   $\epsilon$ .

In summary, the current study shows that the  $\epsilon$  subunit works not only as a regulator but also as an ATP sensor to regulate enzyme activity according to cellular energy status. Studies on the role of ATP binding to the  $\epsilon$  subunit in the ATP synthesis reaction are currently under way.

**Acknowledgments**—We thank Drs. Hiromasa Yagi, Hideaki Tanaka, Tomitake Tsukihara, and Hideo Akutsu and Nobumoto Kajiwar for providing structural information on the ATP binding site of the  $TF_1$   $\epsilon$  subunit.

## REFERENCES

- Boyer, P. D. (1997) *Annu. Rev. Biochem.* **66**, 717–749
- Kinosita, K., Jr., Yasuda, R., and Noji, H. (2000) *Essays Biochem.* **35**, 3–18
- Yoshida, M., Muneyuki, E., and Hisabori, T. (2001) *Nat. Rev. Mol. Cell Biol.* **2**, 669–677
- Senior, A. E., Nadanaciva, S., and Weber, J. (2002) *Biochim. Biophys. Acta* **1553**, 188–211
- Noji, H., Yasuda, R., Yoshida, M., and Kinosita, K., Jr. (1997) *Nature* **386**, 299–302
- Yasuda, R., Noji, H., Kinosita, K., Jr., and Yoshida, M. (1998) *Cell* **93**, 1117–1124
- Smith, J. B., Sternweis, P. C., and Heppel, L. A. (1975) *J. Supramol. Struct.* **3**, 248–255
- Laget, P. P., and Smith, J. B. (1979) *Arch. Biochem. Biophys.* **197**, 83–89
- Ort, D. R., and Oxborough, K. (1992) *Annu. Rev. Plant Physiol. Plant Mol. Biol.* **43**, 269–291
- Kato, Y., Matsui, T., Tanaka, N., Muneyuki, E., Hisabori, T., and Yoshida, M. (1997) *J. Biol. Chem.* **272**, 24906–24912
- Rondelez, Y., Tresset, G., Nakashima, T., Kato-Yamada, Y., Fujita, H., Takeuchi, S., and Noji, H. (2005) *Nature* **433**, 773–777
- Gibbons, C., Montgomery, M. G., Leslie, A. G. W., and Walker, J. E. (2000) *Nat. Struct. Biol.* **7**, 1055–1061
- Rodgers, A. J. W., and Wilce, M. C. J. (2000) *Nat. Struct. Biol.* **7**, 1051–1054
- Richter, M. L., and McCarty, R. E. (1987) *J. Biol. Chem.* **262**, 15037–15040
- Kato-Yamada, Y., Bald, D., Koike, M., Motohashi, K., Hisabori, T., and Yoshida, M. (1999) *J. Biol. Chem.* **274**, 33991–33994
- Kato-Yamada, Y., Yoshida, M., and Hisabori, T. (2000) *J. Biol. Chem.* **275**, 35746–35750
- Tsunoda, S. P., Rodgers, A. J. W., Aggeler, R., Wilce, M. C. J., Yoshida, M., and Capaldi, R. A. (2001) *Proc. Natl. Acad. Sci. U. S. A.* **98**, 6560–6564
- Suzuki, T., Murakami, T., Iino, R., Suzuki, J., Ono, S., Shirakihara, Y., and Yoshida, M. (2003) *J. Biol. Chem.* **278**, 46840–46846
- Iino, R., Murakami, T., Iizuka, S., Kato-Yamada, Y., Suzuki, T., and Yoshida, M. (2005) *J. Biol. Chem.* **280**, 40130–40134
- Kato-Yamada, Y., and Yoshida, M. (2003) *J. Biol. Chem.* **278**, 36013–36016
- Kato-Yamada, Y. (2005) *FEBS Lett.* **579**, 6875–6878
- Yagi, H., Kajiwar, N., Tanaka, H., Tsukihara, T., Kato-Yamada, Y., Yoshida, M., and Akutsu, H. (2007) *Proc. Natl. Acad. Sci. U. S. A.* **104**, 11233–11238
- Iizuka, S., Kato, S., Yoshida, M., and Kato-Yamada, Y. (2006) *Biochem. Biophys. Res. Commun.* **349**, 1368–1371
- Matsui, T., and Yoshida, M. (1995) *Biochim. Biophys. Acta* **1231**, 139–146
- Matsui, T., Muneyuki, E., Honda, M., Allison, W. S., Dou, C., and Yoshida, M. (1997) *J. Biol. Chem.* **272**, 8215–8221
- Ono, S., Hara, K. Y., Hirao, J., Matsui, T., Noji, H., Yoshida, M., and Muneyuki, E. (2003) *Biochim. Biophys. Acta* **1607**, 35–44
- Walker, J. E., Saraste, M., Runswick, M. J., and Gay, N. J. (1982) *EMBO J.* **1**, 945–951
- Higuchi, R., Krummel, B., and Saiki, R. K. (1988) *Nucleic Acids Res.* **16**, 7351–7367
- Ho, S. N., Hunt, H. D., Horton, R. M., Pullen, J. K., and Pease, L. R. (1989) *Gene (Amst.)* **77**, 51–59
- Hisabori, T., Kato, Y., Motohashi, K., Kroth-Pancic, P., Strotmann, H., and Amano, T. (1997) *Eur. J. Biochem.* **247**, 1158–1165
- Landt, O., Grunert, H. P., and Hahn, U. (1990) *Gene (Amst.)* **96**, 125–128
- Stiggall, D. L., Galante, Y. M., and Hatefi, Y. (1979) *Methods Enzymol.* **55**, 308–315
- Bradford, M. M. (1976) *Anal. Biochem.* **72**, 248–254
- Hara, K. Y., Kato-Yamada, Y., Kikuchi, Y., Hisabori, T., and Yoshida, M. (2001) *J. Biol. Chem.* **276**, 23969–23973
- Watanabe, Y.-H., Motohashi, K., and Yoshida, M. (2002) *J. Biol. Chem.* **277**, 5804–5809